

Thermo-mechanical transient analysis of concrete structure around the nuclear reactor

M. Žmindač^{a,*}, P. Novák^a, J. Nozdrovický^b

^a Faculty of Mechanical Engineering, University of Žilina, Univerzitná 1, 010 26 Žilina, Slovak Republic

^b JUNO&PARTNERS ENGINEERING, Ltd.

Received 10 September 2008; received in revised form 20 November 2008

Abstract

This paper deals with transient thermal — stress analysis of concrete structure around the nuclear reactor loaded by dead load and thermal loads. The FEM simulations were performed for various input materials characteristic of concrete based on experimentally obtained physical-mechanical properties and measuring of temperatures. The proposed calculation model, procedures of numerical simulation have been describing conclusions of analysis. The numerical simulation has been performed by means of the finite element method (FEM) using a commercially available ANSYS code.

© 2008 University of West Bohemia in Pilsen. All rights reserved.

Keywords: nuclear reactor, concrete structure, transient thermal-stress analysis, finite element method

1. Introduction

Thermal effect evaluation of concrete structures in nuclear power plants (NPP) is important factor for the plant life management strategy considering ageing of the concrete during plant operation. Rheological properties of the concrete result in creeping and strain release in time, depending on degradation processes, environment humidity, temperature and corrosion rates on steel surface [1]. Its solution is expected to provide a new knowledge about thermally influenced reinforced-concrete structures, i.e. knowledge that is inevitable for the lifetime extension process of nuclear facilities. Individual analyses serve as input for optimal selection of possibilities for increasing the safety and serviceability of concrete elements [2]. Based on simulation results, it will be possible to predict the functionality of concrete structures under potential extreme impacts encountered in NPP and to define dominant degradation processes in the most exposed location from the standpoint of ageing. For getting a more accurate image of the actual behaviour of the structure, it's necessary to consider all mentioned factors for a change of physical and mechanical properties as well as to model the course of load in time.

The paper is aimed at lifetime increasing of reactor pit concrete structure (RPCS) of VVER440 in the power generation industry. Only linear calculation models are applied for simulation of the behaviour of concrete structure around nuclear reactor. Geometrical model of the structure is obtained from CAD system Pro/Engineer and by IGES file is transformed into FEM software ANSYS and finite elements mesh has been generated.

Next goal of this work is generation of reliable FEM model, which is possible to solve on available PC hardware. At last is necessary to verify potential impacts of extreme as well as operating conditions on the structure under thermal effects.

*Corresponding author. Tel.: +421 415 132 962, e-mail: Milan.Zmindak@fstroj.uniza.sk.

2. Theoretical background

The governing equation for transient thermal analysis is [3]

$$\rho c_p \left(\frac{\partial T}{\partial t} + \mathbf{v} \cdot \nabla T \right) - \nabla \cdot (k \nabla T) = q_B \quad \text{on } \Omega, \quad (1)$$

where ρ is density, c_p is specific heat at constant pressure, T is temperature, \mathbf{v} is velocity vector of differential control volume, ∇ is nabla operator, k is thermal conductivity coefficient, \mathbf{q} is heat flux vector and q_B is heat generation rate per unit volume. The boundary and initial conditions have to be added to (1) for uniqueness of solution.

Using principle of virtual temperatures on (1) we obtain governing equation in matrix form

$$\mathbf{C}^t \dot{\mathbf{T}} + (\mathbf{K}^{tm} + \mathbf{K}^{tb} + \mathbf{K}^{tc}) \mathbf{T} = \mathbf{Q}^f + \mathbf{Q}^c + \mathbf{Q}^g, \quad (2)$$

where \mathbf{C}^t is thermal capacity matrix, \mathbf{K}^{tm} is mass transport conductivity matrix, \mathbf{K}^{tb} is diffusion conductivity matrix, \mathbf{K}^{tc} is convection surface conductivity matrix, \mathbf{T} is temperature vector, \mathbf{Q}^f is mass flux vector, \mathbf{Q}^c is convection surface heat flow vector, \mathbf{Q}^g is heat generation load vector.

Applying the variational principle to governing equations of elastic continua and using thermoelastic constitutive equations [4] we obtain element matrix equation for strong coupled thermo-elastic problem

$$\begin{bmatrix} \mathbf{M} & \mathbf{0} \\ \mathbf{0} & \mathbf{0} \end{bmatrix} \begin{Bmatrix} \ddot{\mathbf{U}} \\ \ddot{\mathbf{T}} \end{Bmatrix} + \begin{bmatrix} \mathbf{C} & \mathbf{0} \\ \mathbf{C}^{tu} & \mathbf{C}^t \end{bmatrix} \begin{Bmatrix} \dot{\mathbf{U}} \\ \dot{\mathbf{T}} \end{Bmatrix} + \begin{bmatrix} \mathbf{K} & \mathbf{K}^{ut} \\ \mathbf{0} & \mathbf{K}^t \end{bmatrix} \begin{Bmatrix} \mathbf{U} \\ \mathbf{T} \end{Bmatrix} = \begin{Bmatrix} \mathbf{F} \\ \mathbf{Q} \end{Bmatrix}, \quad (3)$$

where \mathbf{M} is element mass matrix, \mathbf{C} is element structural damping matrix, \mathbf{K} is element stiffness matrix, \mathbf{U} is displacement vector, \mathbf{F} is structural load vector, \mathbf{K}^t is element diffusion conductivity matrix, \mathbf{Q} is thermal load vector (summation of all vectors on right side (2)), \mathbf{K}^{ut} is element thermo-elastic matrix, \mathbf{C}^{tu} is element thermo-elastic damping matrix.

We note that if interaction between coupled fields has a low degree of nonlinearities, then it is possible to solve weak coupled thermo-elastic problem. This type of coupling is more efficient and flexible and therefore was used in our analysis. In this case $\mathbf{K}^{ut} = \mathbf{C}^{tu} = \mathbf{0}$ and for undamped system $\mathbf{C} = \mathbf{0}$. The weak coupling may be shown in the most general form

$$\begin{bmatrix} \mathbf{K}_{11}(\mathbf{X}_1, \mathbf{X}_2) & \mathbf{0} \\ \mathbf{0} & \mathbf{K}_{22}(\mathbf{X}_1, \mathbf{X}_2) \end{bmatrix} \begin{Bmatrix} \mathbf{X}_1 \\ \mathbf{X}_2 \end{Bmatrix} = \begin{Bmatrix} \mathbf{F}_1(\mathbf{X}_1, \mathbf{X}_2) \\ \mathbf{F}_2(\mathbf{X}_1, \mathbf{X}_2) \end{Bmatrix} \quad (4)$$

Then calculation involves two analyses, each belonging to a different physical field. Coupling is made by applying results from one analysis as loads to next analysis.

3. FEM model and solution

Finite element method (FEM) is well adapted to the computation of stresses and strains due to temperatures. A process of computation can be divided into two steps. First, the temperatures are determined as a function of time. Then, the mechanical computation use previous results to get displacements (at nodes) and stresses (at integration points of finite elements). Generally, for practical reasons, used mesh for the heat transfer computation is also the same as for the mechanical analysis. However, the main difficulty comes from the extreme high gradients around the heat source for the temperature and consequently for the stresses. A standard procedure when applying FEM consists of several mutually linked steps.

The first and basic step was to establish the model geometry. In regard to that concrete structure represents complicate structure creation of a realistic model with correct boundary conditions takes much time. The mesh quality can have a considerable impact on the computational analysis with regards on reliable results of solution and computing time. This aspect is especially important if transient analysis is considered. From this point of view, the quality of mesh generation is very important because it provides some indication of how suitable a particular discretization is for the considered analysis type. Different types of elements have been used for generation of FEM mesh.

In this simulation was performed realistic response of structure on static and temperature loadings and their effect on carrying capacity of concrete structure. Regarding to an interaction of reactor with surrounding structure, numerical modelling includes:

1. Static analysis of concrete structure loaded by self-weight.
2. Transient thermal linear analysis.
3. Calculation of thermal stresses.
4. Evaluating the limiting state of structure.

3.1. Geometric model and FEM mesh

Generated model satisfy symmetric boundary conditions (fig. 1), as far as unessential parts of concrete structure and reactor pressure vessel (RPV) are neglected. Geometric model of structure was created in CAD system Pro/Engineer and imported through IGES files into ANSYS program. As mentioned before thermo-elastic coupled problem is solved. Large attention was focused on selection of suitable finite elements types, mesh density, defining static and geometric boundary conditions.

Simulation has been carried out for input material characteristics of concrete, pressure vessel, liner and other steel parts (tab. 1). Materials of concrete structure have been assumed as homogenous isotropic continuum. Finite element mesh was generated mainly using 8-nodes solid elements SOLID70 for thermal analysis and SOLID45 for stress analysis. Whole structure

Table 1. Material properties

	E [GPa]	ν [-]	α [K ⁻¹]	ρ [kg · m ⁻³]	c [J · kg ⁻¹ · K ⁻¹]	λ [W · m ⁻¹ K ⁻¹]
Steel parts	210	0.3	1.2 ⁻⁵	7 850	434	58
Lithium crushed material	0.3	0.3	1.4 ⁻⁵	6 000	880	20
Concrete parts	30	0.15	1.2 ⁻⁵	2 300	820	3.2
Concrete serpentine	20	0.15	1.2 ⁻⁵	3 500	995	4.5
Reactor pressure vessel	200	0.3	1.25 ⁻⁵	7 800	525	36.3
Liner	200	0.3	1.2 ⁻⁵	7 850	440	54.5

E – Young’s modulus, ν – Poisson number, α – thermal expansion coefficient, ρ – density, c – specific thermal capacity, λ – specific thermal conductivity

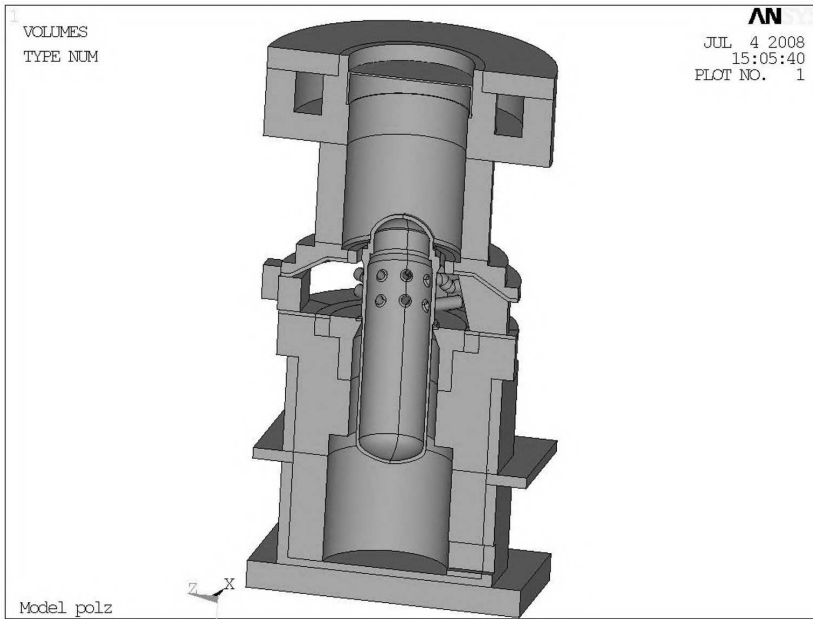


Fig. 1. Geometric model

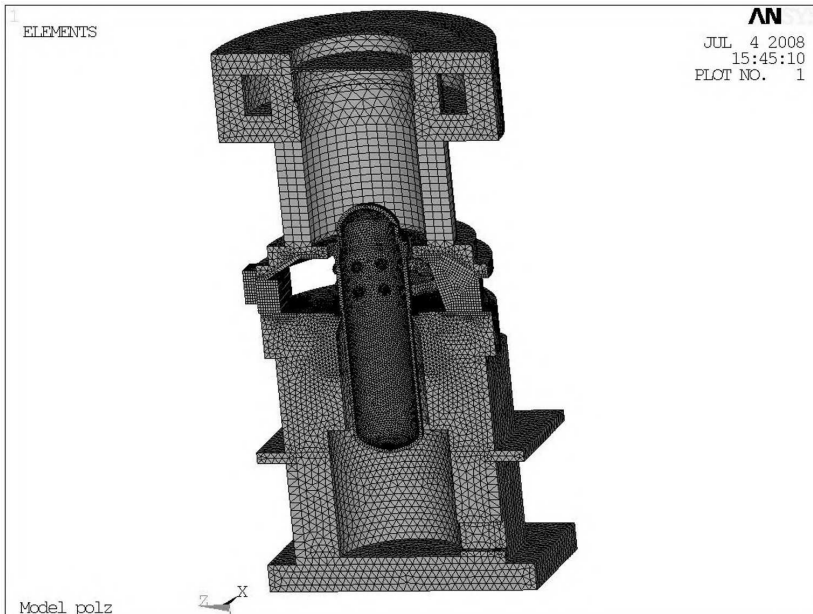


Fig. 2. Finite element mesh

of hermetic zone (walls, floors, top walls) is covering by steel liner from inner side, which safeguards it's tightness. Liner thickness is 8 mm and for discretization shell elements SHELL132 were used for thermal analysis and SHELL181 for stress analysis. We note that before computation of displacement and stress fields, it is necessary to convert thermal finite elements back in

to corresponding structural finite elements. Dilatation of structure was developed due to heating of it, so it was necessary to assure relative motion of concrete parts in location with large temperature gradients. We note that RPV is seated by collar on support, mounted on supporting frame of pit reactor structure. Support consists from support ring, sliding surfaces, splice plates, wedges and fixing parts. Therefore, contact was modelled between: lower part of reactor and concrete supporting members (supporting members), upper part of reactor and collar of RPV, supporting ring and concrete part of pit reactor structure. The contact elements CONTA173 and TARGE170 were used in simulation. The friction coefficient $f = 0.8$ between contact surfaces has been taking to a consideration.

3.2. Boundary conditions

Previous analyses showed that it's very important to define correct boundary conditions [6]. For thermo-mechanical analysis is necessary to define thermal and structural boundary conditions. Because structural boundary conditions are more simply, we first describe them. At first assumption of symmetric boundary conditions for whole structure is accepted. This assumption strongly reduces the size of the FE-model, CPU time and disc memory needed. Then all degrees of freedom (DOF) are fixed on bottom of base plate in y direction. So that boundary conditions satisfied static determinateness are fixed DOF of base plate in corner nodes. Concrete structure is loaded by self-weight and pressure in RPV.

Boundary conditions for transient thermal analysis are more complicated. Start-up of reactor on operating temperature is given by prescribed temperatures on inner surface of RPV according to measured time courses (fig. 3, curve RPV) and on concrete cylinder part (fig. 3, inner wall). To take into account heat transfer by convection it is important to put real values of specific heat transfer (heat transfer coefficient) between flow medium and RPV wall and between RPV wall and environment (free convection). Large amount of experimental data in heat flow was assembled in recent years. However, these are published only for some flow type and flow conditions. It is possible to utilize these data for determination of specific heat transfer coefficient values [7]. In fact, heat transfer coefficient between RPV outer surface is temperature dependent and temperature of environmental air is variable, too. In our case a constant heat transfer coefficient in places of contact with ground $h = 40 \text{ [W} \cdot \text{m}^{-2}\text{K}^{-1}]$ and $h = 38 \text{ [W} \cdot \text{m}^{-2}\text{K}^{-1}]$ for RPV outer surface was considered. For heat transfer between upper surfaces of pull support and inner wall, cylindrical surfaces of liner near to RPV heat transfer coefficient $h = 25 \text{ [W} \cdot \text{m}^{-2}\text{K}^{-1}]$ was considered. For reverse sides of concrete supporting member and pull support, top cover and environment air $h = 10.5 \text{ [W} \cdot \text{m}^{-2}\text{K}^{-1}]$ was considered.

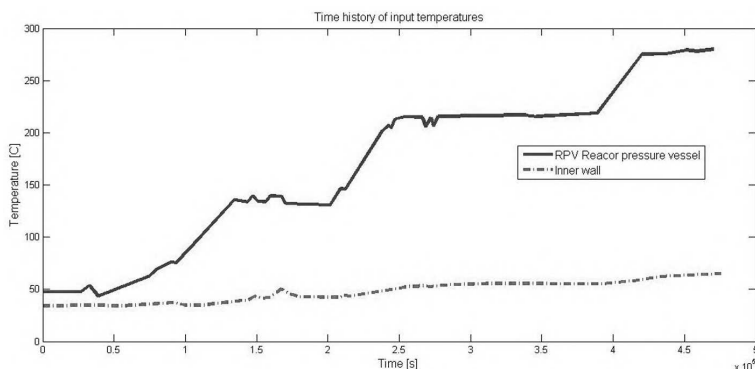


Fig. 3. Time function, temperature [C] – time [s] × 10⁵

3.3. Solution techniques

For assurance heat transfer between contact surfaces it is necessary to execute structural static analysis with contact conditions and dead loading before thermal analysis. Then transient thermal analysis is executed. The displacements and stresses are computed by using linear pseudo-transient analysis with neglecting inertial effects. We note that temperature field computed in thermal analysis is used for calculation of volume loads in dynamic analysis.

4. Simulation and results

The results of numerical simulations are basis for examination of reliability of whole structure or it is possible to qualify only selected part of structure [5]. As pointed out above first analysis of temperature field has been executed. In fig. 4 temperature a field of structure at the end of thermal analysis is described. Maximum temperature reaches value 250 °C at RPV. Graph of temperature vs. time is given in fig. 5 at nodes $U1$ to $U3$ and temperature field in concrete supporting member is given in fig. 6. Maximum temperature values are: $U1 = 185$ °C, $U2 = 100$ °C, $U3 = 80$ °C. Node $U1$ is the closest point to pressure vessel. Node $U3$ is approximately in the middle of concrete supporting member. Maximum temperature in concrete supporting member is 80.116 °C. In fig. 7 is time course of temperatures at nodes $U1$ to $U3$. We can observe from simulation results that high temperatures are occurred in relative small region and they do not reach values in concrete masonry. So that case of temperature increase is excluded at RPCS.

As we mentioned structure stress calculation was executed in two steps. The goal of analysis was checking the allowable stress in concrete supporting member on the basis of evaluated

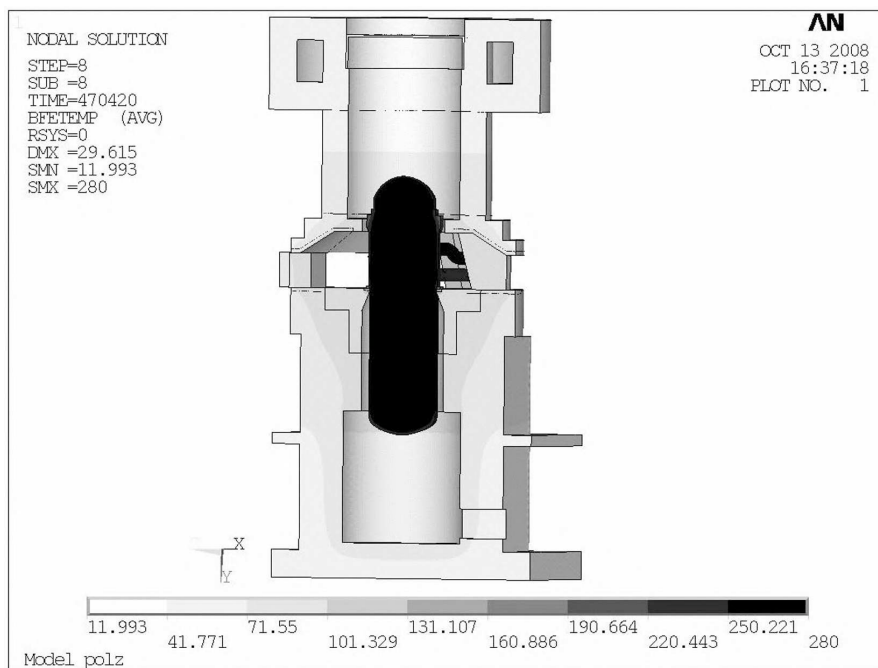


Fig. 4. Stress field at the end of heating

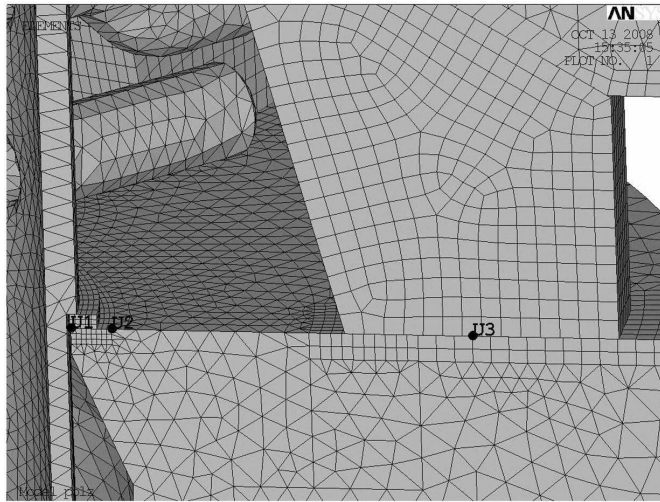


Fig. 5. Node locations for temperatures

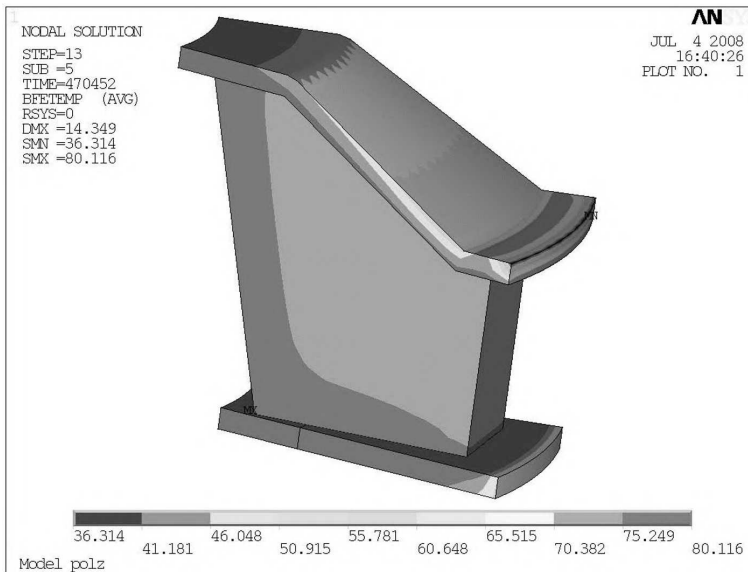


Fig. 6. Temperature field in concrete supporting member

stresses in integration points of finite elements. In fig. 8 stress intensity field is shown

$$\sigma_i = \max(|\sigma_1 - \sigma_2|, |\sigma_2 - \sigma_3|, |\sigma_3 - \sigma_1|) \quad (5)$$

and its maximum value is 21.013 MPa. From numerical results are evaluated stresses at node points as main stresses in tension and at press for nodes is $U1$ to $U4$ (fig. 9). The stresses values at the end of heating are given in tab. 2. Maximum value of main stress in tension is $\sigma_1 = 0.104602$ MPa at node $U4$ and maximum value of main stress in compression is $\sigma_3 = -6.95284$ MPa at node $U3$. Allowable stress of used concrete C25/30 in compression is $f_{cm} = -33$ MPa and average strength in tension is $f_{cmt} = 2.6$ MPa [8].

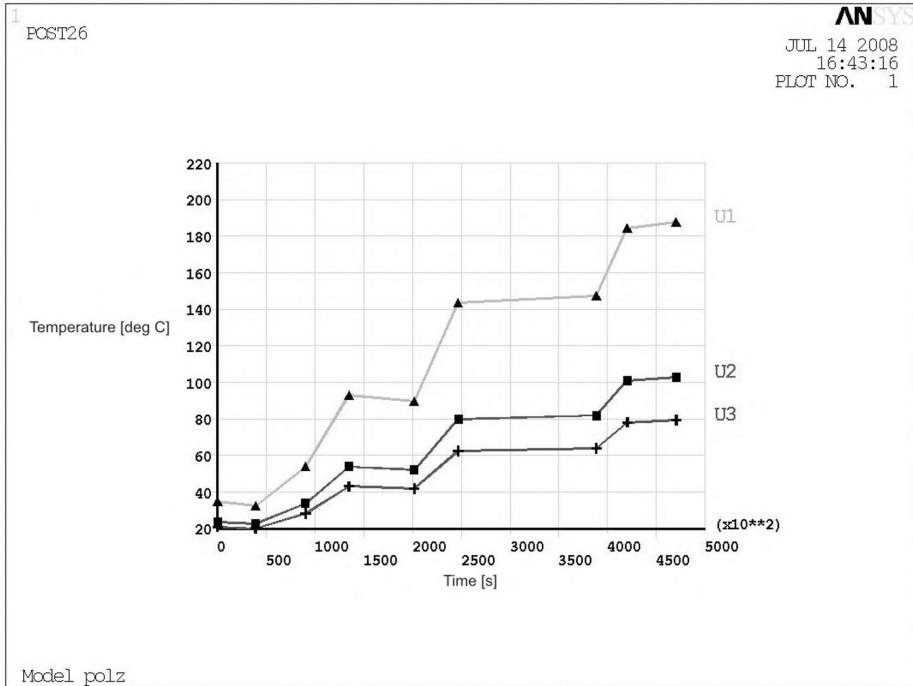


Fig. 7. Temperature field in selected nodes

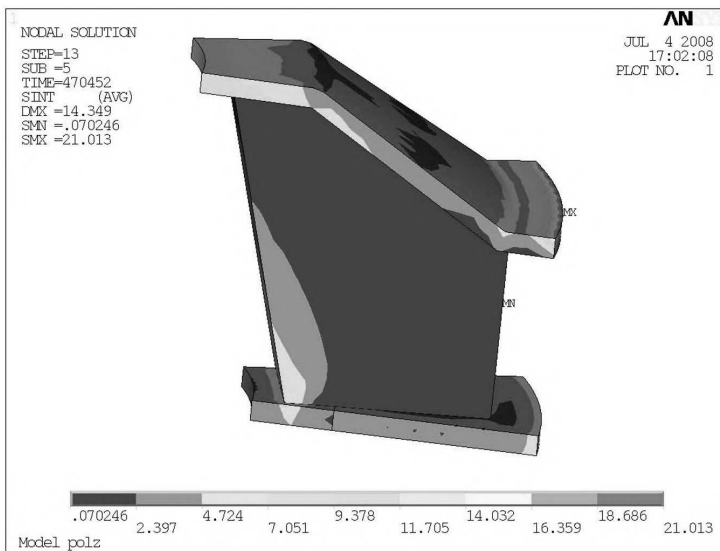


Fig. 8. Stress intensity

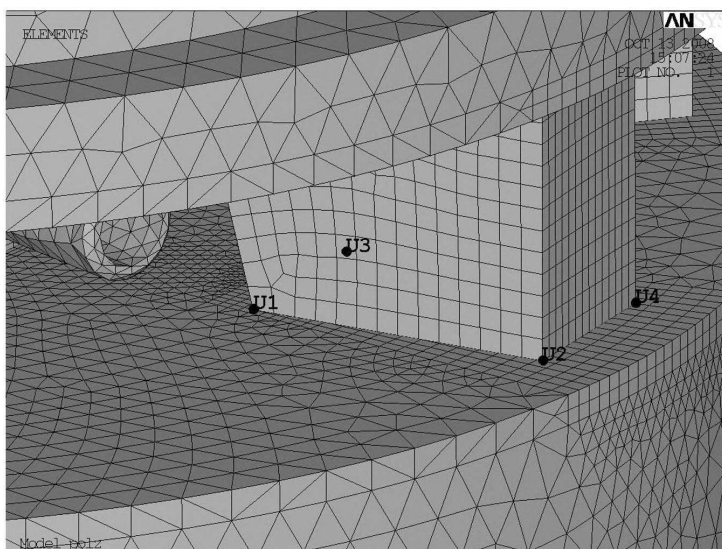


Fig. 9. Node locations for stresses

Table 2. Values of main stress in concrete supporting member [MPa]

Main stresses	Nodes			
	$U1$	$U2$	$U3$	$U4$
σ_1	-0.655 269	0.100 779	-0.804 218	0.104 602
σ_2	-1.736 67	-0.209 189	-2.052 04	-0.209 279
σ_3	-6.025 06	-0.609 500	-6.952 84	-0.612 427

5. Conclusion

This paper deals with the thermo-elastic analysis of RPCS around the nuclear reactor for individual load types using FEM commercial program ANSYS 11.0. Three-dimensional FE model was used in numerical simulation of RPCS and non-stationary conditions of heat transfer were considered. These conditions are incoming immediately after running of reactor. Solving weak coupled thermo-elastic problem were determined values of displacements, deformations, stresses and internal forces in the whole concrete structure. Effects from static and thermal loads on RPCS were analyzed particularly. Largest temperatures are reached near by of RPV. So that accumulation of high temperatures is relatively at small region and do not interfere into concrete massif. We note that on base experiences of concrete experts is not necessary to accept none arrangements as far as temperature in concrete not exceed 100 °C.

In strength analysis were evaluated only stresses in selected part of structure, at concrete supporting member. The results are summarized in tab. 2. As we consider that average strength of used concrete C25/30 in compression is $f_{cm} = 33$ MPa and average strength in tension is $f_{cmt} = 2.6$ MPa, then we can state that concrete structure meets according to method of allowable stress. In conclusion it is possible to state that concrete structure meets static and thermal effects.

In future research we will consider examination of critical cross-sections by limit deformation method according to STN P ENV 1992-1-6. It should be contribution to complex analysis of the buildings of NPP from the point of view of their resistance to possible accidents. Taking into account the fact that these are systems with stochastic character and likewise their degradation is of stochastic character, the aim of all modern approaches to the evaluation of complex reliability of structures will be use probabilistic methods of solution.

Acknowledgements

The work has been supported by the grant project of Slovak Agency for Research and Development (grant No. APVV-99-005305).

References

- [1] O. B. Isgor, A. G. Raapur, Modelling steel corrosion in concrete structures. *Materials and Structures* 39 (2006) 291–302.
- [2] A. R. Chini, L. Acquaye, Effect of elevated curing temperatures on strength and durability of concrete. *Materials and Structures* 38 (2005) 673–679.
- [3] G. Dhondt, *The Finite Element Method for Thermo-mechanical Applications*, John Wiley and Sons, Ltd., 2004.
- [4] Theory reference for ANSYS and ANSYS Workbench, ANSYS Release 11, ANSYS Inc., 2007.
- [5] J. Králik, J. Králik, Jr., Probability and sensitivity analysis of interaction of tower building CBC with background, *Proceedings of ANSYS User's Meeting, Tábor, 2006* (in Slovak).
- [6] M. Žmindák, J. Nozdrovický, J. Mazúr, Thermo-mechanical analysis of reinforced concrete structure. *Proceedings of Mechanical Engineering 2007, STU Bratislava, 2007* (in Slovak).
- [7] D. Bobok, K. Jelemenský, *Theory of mater transmissions*, STU Bratislava, 2006 (in Slovak).
- [8] Z. Hroncová, M. Moravčík, *Concrete structures: Dimensioning on base STN P ENV 1992-1-1, Žilinská univerzita v Žiline, 2005* (in Slovak).